AIChE J, 12, 35 (1966).
Furusawa, T., and J. M. Smith, "Fluid-Particle and Intraparticle Mass Transport Rates in Slurries," *Ind. Eng. Chem. Fundamentals*, 12, 197 (1973).
Grant, H. L., R. W. Stewart, and A. Moilliet, "Turbulence Spectra from a Tidal Channel," *J. Fluid Mech.*, 12, 241 (1962).
Günkel, A. A., "Flow Phenomena in Stirred Tanks", Ph.D. thesis, McGill University, Montreal, Canada (1973).
———., R. P. Patel, and M. E. Weber, "A Shielded Hot-Wire Probe for Highly Turbulent Flows and Rapidly Reversing Flows," *Ind. Eng. Chem. Fundamentals*, 10, 627 (1971).
Harriott, Peter, "Mass Transfer to Suspended Particles: Part I. Suspended in Agitated Tanks," *AIChE J.*, 8, 93 (1962).
Hinze, J. O., *Turbulence*, McGraw-Hill, New York (1959).
Humphrey, D. W., and H. C. van Ness, "Mass Transfer in a Continuous Flow Mixing Vessel," *AIChE J.*, 3, 283 (1957).
Kim, W. J., and F. S. Manning, "Turbulence Energy and Intensity Spectra in a Baffled Stirred Tank," *AIChE J.*, 10, 747 (1964).
Levins, D. M., and J. R. Glastonbury, "Particle—Liquid Hydrodynamics and Mass Transfer in a Stirred Vessel; Part I—Particle—Liquid Motion," *Trans. Inst. Chem. Engrs.*, 50, 32 (1972); "Part II—Mass Transfer," *ibid.*, 132.
Manning, F. S., and R. H. Wilhelm, "Concentration Fluctuations in a Stirred, Baffled Vessel," *AIChE J.*, 9, 12 (1963).
Miller, D. N., "Scale-up of Agitated Vessels," *Ind. Eng. Chem. Proc. Design Develop.*, 10, 365 (1971).
Mujumdar, A. S., B. Huang, D. Wolf, M. E. Weber, and W. J. M. Douglas, "Turbulence Parameters in a Stirred Tank," *Can. J. Chem. Eng.*, 48, 475 (1970).
O'Connell, F. P., and D. E. Mack, "Simple Turbines in Fully Baffled Tanks—Power Characteristics," *Chem. Eng. Progr.*, 46, 358 (1950).
Rao, A. M., and R. S. Brodkey, "Continuous Flow Stirred Tank Turbulence Parameters in the Impeller Stream," *Chem. Eng. Sci.*, 27, 137 (1972).
Reith, I. T., "Generation and Decay of Concentration Fluctuations in a Stirred, Baffled Vessel," *AIChE Symposium Series No. 10*, 14 (1965).
Sato, Y., Y. Horie, M. Kamiwano, and K. Yamamoto, "Turbulence Flow in a Stirred Vessel," *Kagaku Kogaku*, 31, 79 (1967).
Schwartzberg, H. G., and R. E. Treybal, "Particle and Fluid Motion in Turbulent Stirred Tanks—Fluid Motion", *Ind. Eng. Chem. Fundamentals*, 7, 1 (1968).
Uhl, V. W., and J. B. Gray, ed., *Mixing—Theory and Practice*, Vol. 1, Academic Press, New York (1966).

Manuscript received June 10, 1974; revision received and accepted April 30, 1975.

Mixing in the Interaction Zone of Two Free Jets

Mixing in the interaction zone of two round free jets with nozzle axes intersecting at half-angles of 15, 30, and 45 deg. has been studied by the smoke scattered light technique. The fields of mean concentration and concentration fluctuation intensity were mapped with one jet marked with smoke, the other jet marked, and both jets marked. The correlation function between the concentration fluctuations associated with fluid of the two nozzle streams has been calculated from the results and is an important characteristic of the mixing field and a significant measure of molecular mixedness. A transport equation for the associated covariance function is derived, and the special features of the mathematical modeling problem for this class of mixing process are discussed. The implications of the results for processes involving chemical reactions are examined.

H. A. BECKER and B. D. BOOTH

Department of Chemical Engineering
Queen's University
Kingston, Ontario, Canada

SCOPE

Rapid and thorough mixing of fluid streams is often accomplished by means of turbulent jets. The mixing may be accomplished by chemical reaction, as in combustion systems where some or all of the jets may take the form of turbulent diffusion flames. In either case, with or without chemical reaction, knowledge of the turbulent mixing process is essential to an understanding of the system performance. The present work is a contribution towards such knowledge in two areas of higher complexity on which published data are meager: mixing fields entered by three or more feed streams and mixing fields with a strongly three-dimensional character. Experimental results are reported for a typical and practically significant example. A theoretical analysis of the special features of the three-stream problem is given and is applied to interpret the experimental data.

The situation chosen for experimental study is that of two jets (both air) issuing into a virtually infinite, stagnant body of fluid (room air). The nozzle axes are coplanar and intersect in the downstream direction; that is, the jets are obliquely aimed towards each other. The angle 2α between the axes was given values of 30, 60, and 90 deg. Interest was focused on the interaction zone where the jets merge and the nozzle fluid from each becomes thoroughly mixed with that of the other. A light-scatter technique was used to study the mixing process. First one nozzle stream was marked with smoke, then the other, and finally both. Measurements were made of the mean (time-average) smoke concentration field and of the root-mean-square value, called the *intensity*, of the turbulent con-

Correspondence concerning this paper should be addressed to H. A. Becker. B. D. Booth is with the Department of Consumer and Corporate Affairs, Government of Canada, Ottawa, Canada.

centration fluctuation. Previous work has shown that the smoke used is an adequate marker for these measurements, and its concentration field models the concentration field of the marked gas stream to the required degree of faithfulness.

The theoretically most interesting and novel aspects of the problem pertain to the superposition properties of the concentration fields of material from the two nozzle streams in the interaction zone. These properties are analyzed, and their role in the mathematical description of the mixing process is established. The implications for chemical reactions between the streams are also examined.

CONCLUSIONS AND SIGNIFICANCE

The two jets, before meeting, are strongly deflected towards each other, but apart from this they behave much like isolated free jets. At values of the half-angle of intersection α around 45 deg. (nozzle axes at right angles), there is a relatively stagnant back mixing zone between the jets where they meet. The key length scale for the system is the distance L from the point of jet origin to the point P of intersection of the nozzle areas, roughly the distance to P from either of the nozzle mouths. The length of the jet interaction zone is approximately L. At the end of this zone, the material from the two nozzle streams is fully mixed, and the process occurring thereafter is the further jet mixing of this mixture with entrained ambient fluid.

The experimental information from the work is summarized in a set of mappings of the fields of mean concentration and concentration fluctuation intensity for the jet interaction zone, all presented in a generalized nondimensional form. The principal theoretical findings relate to the covariance between concentration fluctuations in material from the two nozzle streams and to the associated correlation function R_{12}. This covariance function arises naturally in the mathematical description of the mixing field, and its transport (conservation) equation has been derived. It also arises in connection with chemical reactions between material of the nozzle streams. The value of R_{12} ranges from -1 for the unmixed state, where the jets first meet, to $+1$ for the completely mixed state, at the end of the interaction zone where the material of the two nozzle streams has become perfectly mingled. Thus R_{12} is an excellent index for the extent of mixing between any two streams in a multistream mixing problem. It also indicates the extent of reaction in the case of a mixing-limited chemical reaction between the two streams.

The system consisting of two interacting jets has important applications, particularly in combustion, and poses interesting problems of turbulent mixing. Experimental investigations have been few, however, partly, no doubt, because the field is three dimensional. One of the earliest studies was by Rummel (1937) who measured the field of mean concentration of the jet nozzle fluid. The angle between the axes of the round nozzles was varied between 0 and 90 deg. His results indicate that the mixing volume needed to achieve the same dilution with entrained ambient fluid decreases with increasing value of the angle of intersection.

Makaroff and Khudenko (1965) and Kirillov and Khudenko (1965) examined the direction taken by the jet resulting from the interaction of two others. Baron and Bollinger (1952) studied the mean velocity fields of interacting jets, primarily to test the validity of the superposition principle in respect to solutions of the equations of motion under the Reichardt hypothesis for turbulent transport. The principle was found to be usefully accurate only at small angles of intersection.

The aspects of the two-jet mixing problem that are often of greatest practical interest are connected with the field of chemical composition in the interaction region. Both the mean composition and the turbulent inhomogeneities may be important. In the present work the light-scatter technique developed first by Rosensweig et al. (1961) and subsequently by Becker et al. (1967*b*) was applied, facilitating study of both the mean value and the turbulent fluctuations in the concentration of nozzle fluid.

Besides providing performance data on an interesting system and new insights into turbulent mixing processes, the present results should be useful in the effort to develop prediction methods for three-dimensional turbulent flows. A field of strongly interacting free turbulent shear flows poses a reasonably difficult challenge, and success in treating the situation may be regarded as a fairly rigorous test for both computation procedures and turbulent transport

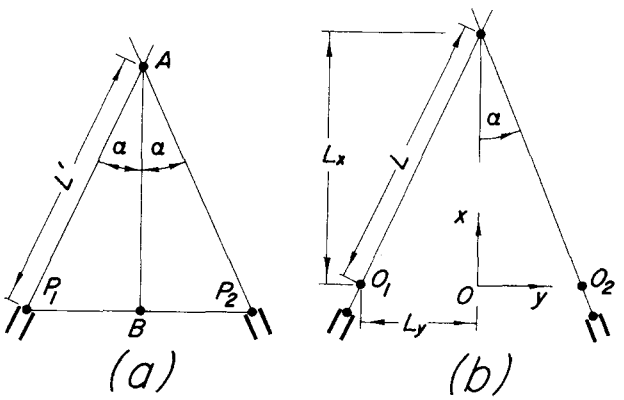

Fig. 1. Geometry of interacting jets in the present case; nozzles with their axes in the same plane, and with their discharge openings at the same distance from the point of intersection of the axes. The points O_1 and O_2 are the virtual origins of the jets.

hypotheses. The light-scatter technique yields data of uniformly high accuracy, in regions of both low and high turbulence intensity, and in regions of whatever flow direction (mainstream or separated). The data are therefore particularly suitable for a critical comparison between prediction and experiment.

SYSTEM PROPERTIES

Outside the development region in the neighborhood of the nozzle, an isolated free jet behaves, in effect, as if it came from a point source where the mass flux is zero but the momentum flux is that, I_o, which crosses the nozzle exit plane. The present interacting jets are expected to exhibit such behavior if $L' >> D$, where $L' \equiv AP_1 = AP_2$, Figure 1*a*. We shall assume that the points of virtual origin, O_1 and O_2, lie on the nozzle axes and at the same distances from the exit planes as if each jet were operating in isolation. A useful and significant representation of the

system geometry is then that illustrated in Figure 1*b*. The configuration is characterized by the half-angle α between the nozzle axes. The characteristic length scale is taken to be $L \equiv O_1A = O_2A$. A Cartesian coordinate system is defined with the origin O at the midpoint O_1O_2, the y axis along O_1O_2, and the x axis along OA. Two auxiliary length scales are available: $L_x = L \cos \alpha = OA$, and $L_y = L \sin \alpha = O_1O = O_2O$.

The jet fluid in the present work was air and the ambient medium was room air, all at the same density ρ. The mass flux from each nozzle was $\dot{m}_o$, and the momentum flux was I_o. The mean discharge velocity was $U_o \equiv \dot{m}_o/\pi\rho R^2$, where $R \equiv D/2$ is the nozzle throat radius. We have

$$I_o = \pi K \rho U_o^2 R^2 \tag{1}$$

where K is the momentum shape factor for the exit velocity profile, with $K = 1$ in the case of a uniform velocity distribution. The nozzles were actually long tubes, so the exit velocity distribution approximated that of an equilibrium pipe flow.

The application of the light-scatter technique to study the nozzle fluid concentration field requires that one or both of the nozzle streams be uniformly marked with smoke. The flux of marker from a nozzle is

$$J_o = \dot{m}_o \Gamma_o/\rho = \pi \Gamma_o U_o R^2 \tag{2}$$

where Γ_o is the marker concentration at the nozzle exit plane.

A generalized representation of the marker concentration field in the interaction zone of the jets requires that concentrations are normalized on a characteristic concentration Γ^*, and that spatial positions are normalized on a characteristic scale L. We have already indicated our choice of L; $L = O_1A = O_2A$ in Figure 1*a*. In order to define an appropriate value of Γ^* for the interaction zone, we require a characteristic stream speed U^*. Dimensional reasoning applied to the basic set of variables $\{I_o, J_o, \rho, L\}$ suggests that

$$U^* \equiv (I_o/\pi\rho L^2)^{1/2} \tag{3}$$

$$\Gamma^* \equiv J_o/\pi U^* L^2 \tag{4}$$

The substitution of (1) and (2) for I_o and J_o gives

$$\Gamma^* = \Gamma_o R/(L\sqrt{K}) \tag{5}$$

The instantaneous marker concentration at any point in the mixing field is Γ, and for a statistically stationary field $\Gamma = \overline{\Gamma} + \gamma$, where $\overline{\Gamma}$ is the mean and γ is the random fluctuation. The generalized representation of the field of $\overline{\Gamma}$ is

$$\overline{\Gamma}/\Gamma^* = f(\mathbf{r}/L, \alpha, Re, Ma, L/D, \text{nozzle shape}, \text{nozzle exit velocity distribution}) \tag{6}$$

where $\mathbf{r} \equiv \mathbf{i}x + \mathbf{k}y + \mathbf{j}z$ is the position vector, $Re \equiv U_oD/\nu$ is the nozzle Reynolds number, and $Ma \equiv U_o/c$ is the nozzle Mach number. We shall consider Re to be large and Ma to be small, so that neither of these parameters significantly affects the mixing process. The effect of Re should, though, be considered as a variable when Re falls below a value somewhere in the range 3 000 to 8 000.

When $L/D >> 1$, the jets behave as if they issued from point sources. With Re large and Ma small, (6) reduces to

$$\overline{\Gamma}/\Gamma^* = f(r/L, \alpha) \tag{7}$$

The nozzles can then be square in throat cross section ($a \times a$) or even rectangular ($a \times b$), and the results will be virtually the same so long as L/a and $L/b >> 1$. Furthermore, the nozzle flow rates and sizes need not be the same, so long as the momentum fluxes I_o are equal.

The field of the intensity of the marker concentration fluctuations $\hat{\gamma} \equiv \sqrt{(\gamma^2)}$ can be represented in the same way as that of $\overline{\Gamma}$. Alternatively

$$\hat{\gamma}/\overline{\Gamma} = g(r/L, \alpha, \ldots) \tag{8}$$

and this is the form that is usually most useful.

EXPERIMENTAL

The nozzles were 32 cm long sections of 0.635 cm I.D. precision bore glass tubing. The feed air to one or both nozzles could be marked with an oil condensation smoke. The air flows to the two nozzles were equal and constant within ± 0.1% variation. The nozzle Reynolds number at the chosen flow rate was 70 000. The momentum parameter K was estimated to be 1.021.

The light-scatter technique is described in other publications (Rosensweig et al., 1961; Becker et al., 1965, 1966, and 1967). The technique allows measurement of the mean concentration of marker, the intermittency factor, and the following properties of marker concentration fluctuations: the intensity, the frequency spectral density function, the autocorrelation function, the two-point spatial correlation function, the integral spatial scale, and others. A very complete characterization of the mixing field was, however beyond the possible scope for the project. It was decided that a careful study of the fields of the mean concentration $\overline{\Gamma}$ and of the concentration fluctuation intensity $\hat{\gamma} \equiv \sqrt{(\gamma^2)}$ would give the best yield of new and useful information. Even here the objectives had to be limited, and the measurements were restricted to the plane of bilateral symmetry containing the nozzle axes (the plane $z = 0$). An exploration of the other plane of symmetry, $y = 0$, would be interesting, but the present results are sufficient to reveal the most significant features of the mixing field.

It has been shown (Becker et al., 1967*b*) that when low-pass filtration of the signal in the light-scatter technique is arranged so that the cutoff wave number is around the value $\kappa = (\epsilon/\nu^3)^{1/4}$ where viscous dissipation of velocity eddies occurs, then the convective aspects of gas mixing are effectively modeled, or, in general, the case $Sc \simeq 1$. The conditions in the present work satisfied this criterion, and hence the field of smoke concentration indeed represented that of nozzle fluid concentration in all the measurements that were made. Due corrections were applied for the effects of finite control volume size, electronic shot noise, and other sources of error as discussed by Becker et al. (1967*b*).

The distance between the nozzle centers $L_{12} \equiv P_1P_2$, Figure 1*a*, was held constant at $L_{12} = 24\,D$. It would have been better, though the results would be very little affected, to have kept L/D constant (see L in Figure 1*b*); then the jets would have had roughly the same development distance up to the interaction zone at all values of α. Three values of the half-angle between the nozzle axes were used: $\alpha = 15$, 30, and 45 deg. Study of the interesting case $\alpha = 90$ deg. (direct opposition of the jets) was precluded by the fact that the smoke would then spill into the room. The case $\alpha = 0$ (parallel alignment) was not investigated either. However, both these cases may be considered in future projects.

The smoke concentration field of the interacting jets was studied first with one nozzle stream marked, then with the other, and finally with both. The concentration field of the jets operating singly was also investigated to determine the location of the virtual jet origin, for comparison with the two-jet field, and for comparison with past work.

RESULTS FOR THE SINGLE FREE JET

The mean concentration field of the single jet was found to be described by

$$b = 0.12\,(x - 10\,R) \tag{9}$$

$$\Gamma_o/\overline{\Gamma}_c = 0.105\,(x - 10\,R) \tag{10}$$

$$\overline{\Gamma}/\overline{\Gamma}_c = \exp(-0.693\,r^2/b^2), \quad r < 2b \tag{11}$$

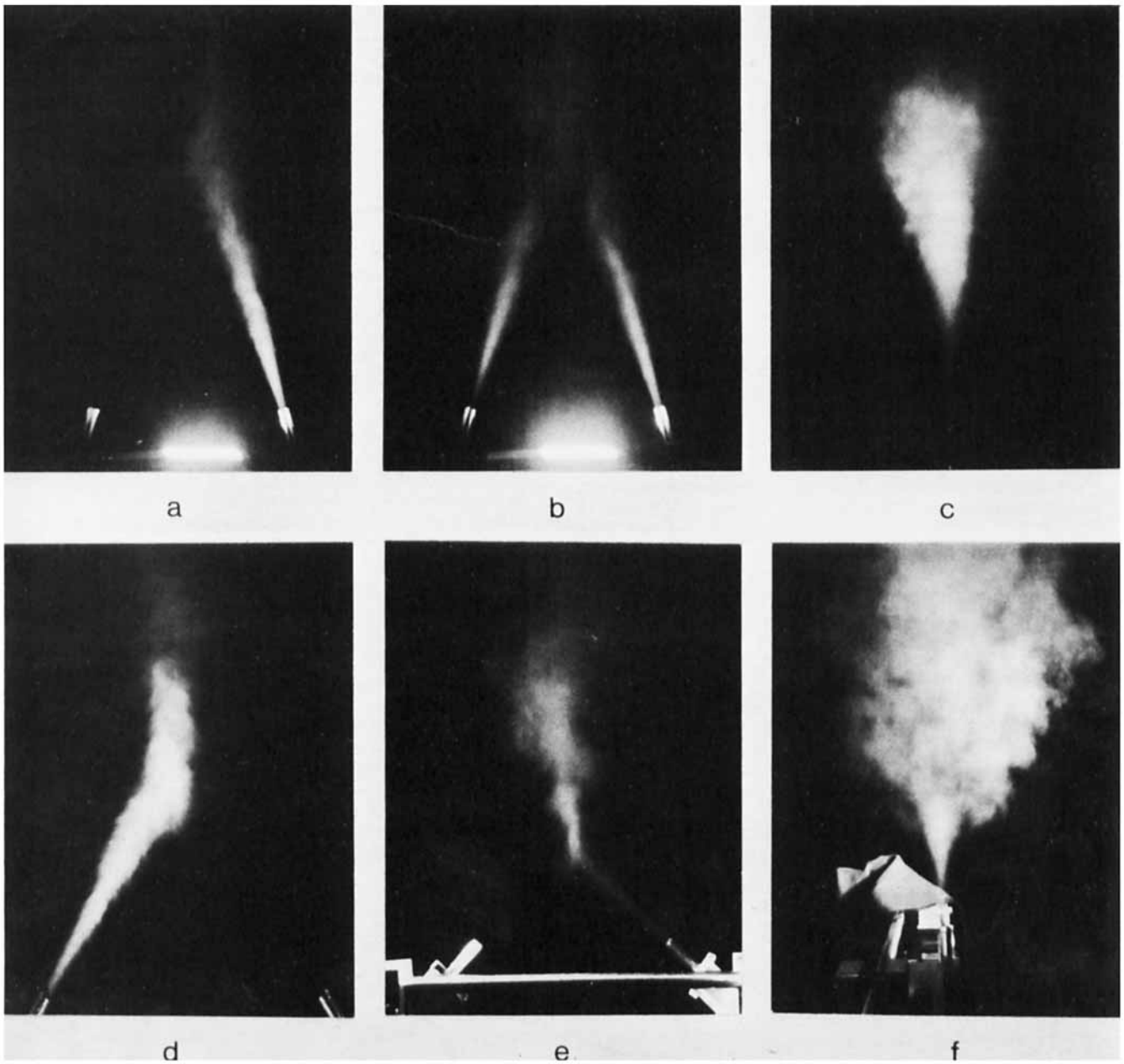

Fig. 2. Photographs of smoke marked jets, by flash illumination. Views *a*, *b*, *d*, and *e* are normal to the plane of the nozzle axes, while *c* and *f* are tangent to this plane. In *b* both jets are marked, while in *a*, *d*, and *e* only one jet is so distinguished. In *c* and *f* the picture is virtually the same for any marking. In *a*, *b*, and *c*, $\alpha =$ 15 deg.; in *d*, 30 deg.; and in *e* and *f*, 45 deg.

where x and r are cylindrical coordinates with origin at the nozzle center, $\overline{\Gamma} = \overline{\Gamma}(x, r)$, $\overline{\Gamma}_c(x) \equiv \overline{\Gamma}(x, 0)$, $r = b(x)$ at $\overline{\Gamma}(x, r) = 1/2\,\overline{\Gamma}_c(x)$.

These results are similar to those of Becker et al. (1967*c*) for a free jet issuing from a flow nozzle providing a uniform exit velocity profile ($K = 1$). The virtual origin of the jet, here at $x = 10\,R$ and there at $x = 4.8\,R$, is, however, nearly twice as far downstream, and this must be attributed to the difference in nozzle geometries. The proportionality constants in (9) and (10) are within the normal range of values reported in the literature, summarized by Becker et al. (1967*c*, Table 3).

The concentration fluctuation intensity on the jet center line was found to be described by

$$\hat{\gamma}_c/\overline{\Gamma}_c = 0.24/(1 + 1.45\,\overline{\Gamma}_c/\Gamma_o) \qquad (12)$$

This is very similar to the result of Becker et al. [1967*c*, Equation (9)].

RESULTS FOR INTERACTING JETS

Photographic Evidence

The mapping of the concentration field of the interacting jets was, as we have said, confined to the plane of bilateral symmetry containing the nozzle axes (the plane $z = 0$). The three-dimensional character of the field can be seen, however, in photographs of the smoke marked jets, Figure 2. These show the expected fanning out of the flow along the plane $y = 0$, and the effect is most dramatic at the largest jet angle of incidence, $\alpha = 45$ deg. In Figure 2*e* a wisp of smoke can be seen extending backwards from the interaction zone; it indicates a recirculation zone, the form of which was clearly revealed by the concentration measurements.

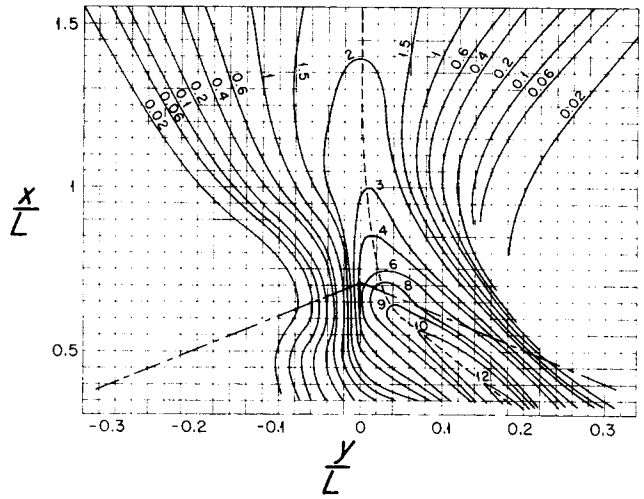

Fig. 3. Field of the normalized mean concentration, $(\overline{\Gamma}_i L/\Gamma_0 R)\sqrt{C}$ with one jet marked, $\alpha = 45$ deg. The dash-dotted lines indicate the nozzle axes. The dashed curve follows the lateral maxima of $\overline{\Gamma}_i$ and is taken to be the jet trajectory as defined by this field.

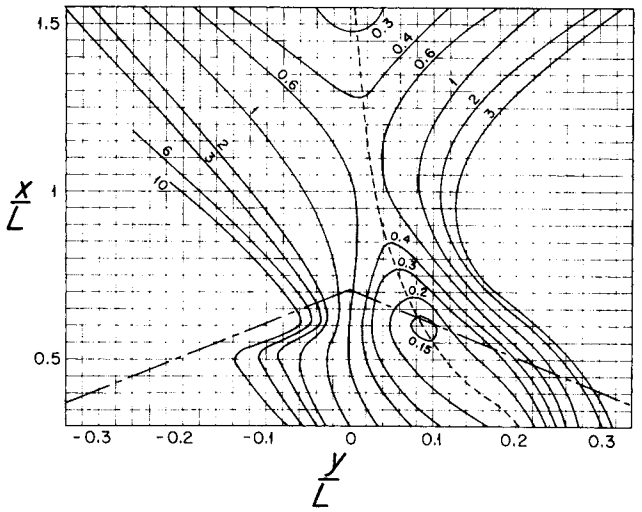

Fig. 4. Field of the relative concentration fluctuation intensity, $\hat{\gamma}_i/\overline{\Gamma}_i$ with one jet marked, $\alpha = 45$ deg. The dash-dotted lines indicate the nozzle axes. The dashed curve follows the lateral minima of $\hat{\gamma}_i/\overline{\Gamma}_i$.

Concentration Profiles and Contour Maps

The concentration field in the plane $z = 0$ at the three values of α, namely, 15, 30, and 45 deg., was mapped by traverses along the y direction at selected values of x. The coordinate system used is that shown in Figure 1*b*, with the virtual jet origins located on the nozzle axes at a distance 10 R from the nozzle planes (as suggested by the study of the single jet).

The profiles so obtained, the set for $\alpha = 30$ deg. is shown in Appendix A*, were used as data for the development of contour maps of the concentration field. These maps were carefully made, and appropriate interpolation and extrapolation techniques were used where necessary in order to delineate the features as accurately as possible. The maps for $\alpha = 45$ deg. are shown in Figures 3, 4, and 5. The set for $\alpha = 15$ deg. is in Appendix A.* It was found, after the project had been terminated, that the data for $\alpha = 30$ deg. were insufficient for this purpose, more data being needed in the critical region $0.5\ L < x < 1.4\ L$. This gap in the results is, however, inconsequential insofar as the general conclusions of the study are concerned.

It should be noted that Figures 3, 4, 5, and 8, and the corresponding figures in Appendix A,* are not quite in the form indicated by (7) and (8) because of a constant numerical error which was equivalent to the use of an incorrect value of the momentum parameter K. We have made an appropriate correction simply by introducing the constant $C = 0.853\ K$.

Jet Trajectories

The contour map of the field of mean concentration with one jet marked, Figure 3, shows a ridge, the crest of which is indicated by the heavy dashed curve. This crest may be termed the trajectory of the marked jet w.r.t. the field $\overline{\Gamma}_i$. Here, and more so at $\alpha = 15$ and 30 deg., it lies so near the curve containing the lateral maxima $\{\overline{\Gamma}_i \mid \partial\overline{\Gamma}_i/\partial y = 0\}$ as to be indistinguishable. A dimensionless representation of this trajectory for all values of α is shown in Figure 6. The normalization used, y/L_y vs. x/L_x, produces a convergence of the data on a single curve at $x < 0.8\ L_x$, and thus suggests a helpful generalization for interpolating between values of α. The other notable feature is that the interacting jets are quite markedly displaced away from

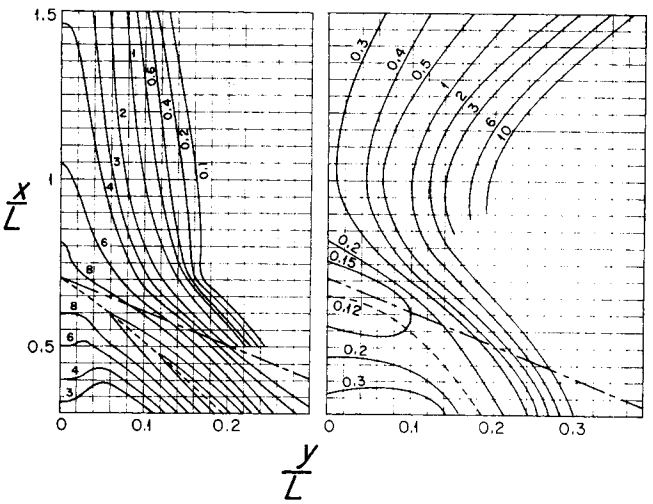

Fig. 5. Concentration field with both jets marked, $\alpha = 45$ deg. Left, $(\overline{\Gamma}L/\Gamma_0 R)\sqrt{C}$, and right, $\hat{\gamma}/\overline{\Gamma}$. The dash-dotted lines indicate the nozzle axes.

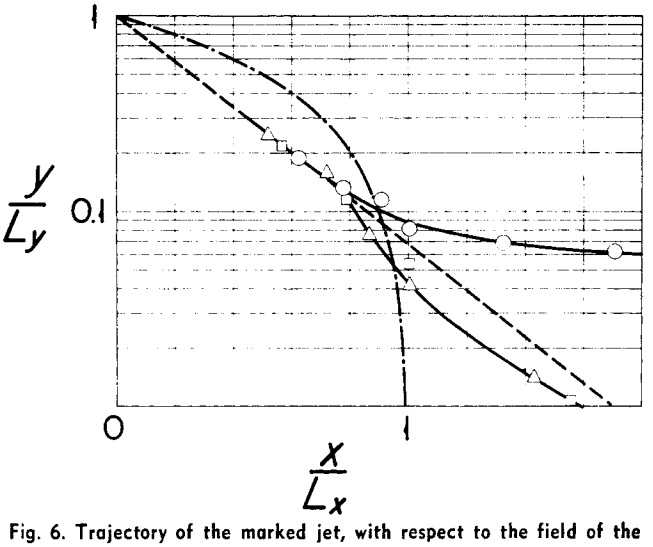

Fig. 6. Trajectory of the marked jet, with respect to the field of the mean concentration $\overline{\Gamma}_i$, one jet marked. The dash-dotted line indicates the nozzle axis. Half-angles of intersection, α: ○, 15 deg.; □, 30 deg.; and △, 45 deg.

* National Auxiliary Publications Service (NAPS) Document No. 02679.

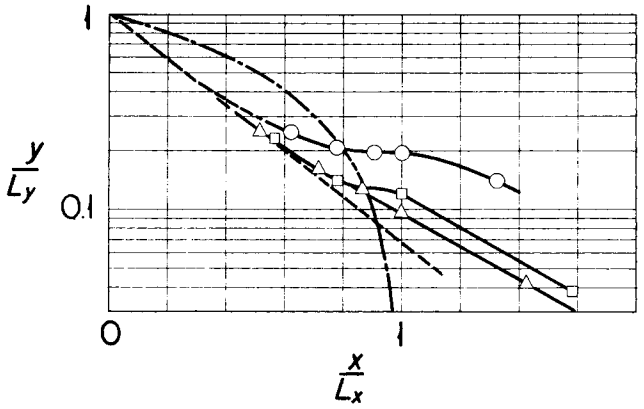

Fig. 7. Trajectory of the marked jet, with respect to the field of the relative concentration fluctuation intensity $\hat{\gamma}_i/\bar{\Gamma}_i$, one jet marked. The dash-dotted line indicates the nozzle axis. Half-angles of intersection, α: ○, 15 deg.; □, 30 deg.; and △, 45 deg.

the nozzle axis, towards each other. This can be explained by the tendency of each jet to entrain fluid from its surroundings which, until the jets effectively merge, acts like a force of mutual attraction between them.

The field of relative concentration fluctuation intensity with one jet marked, $\hat{\gamma}_i/\bar{\Gamma}_i$, also has a trajectorylike feature, Figure 4, a valley whose bottom is closely approximated by the curve of the lateral minima $\{\hat{\gamma}_i/\bar{\Gamma}_i \mid \partial(\hat{\gamma}_i/\Gamma)/\partial y = 0\}$. The trajectories so obtained in Figure 7 differ slightly from those in Figure 6 at $\alpha = 30$ and 45 deg., and more markedly at 15 deg.

Concentration Variation Along the Jet Trajectory

Figure 8 shows the variation of $\bar{\Gamma}_i$, the mean concentration with one jet marked, with distance s along the jet trajectories in Figure 6. The result for the single free jet, Equation (10), also shown is put into the required form by substituting $x - 10\,R = s$ and $K = 1.021$, giving

$$(\bar{\Gamma}_c L/\Gamma_o R)\sqrt{K} = 9.62\,L/s \qquad (13)$$

where L, in this case, has no physical significance. The data for the interacting jets converge with (13) at small values of s/L, as expected, and the differences remain small up to $s/L = 1$. In the range $1 < s/L < 2$, the dilution per unit distance is much more rapid than in the single jet. Beyond $s/L = 2$, the interacting jets appear to have effectively merged and are entering the final regime of the system's mixing history.

Figure 9 shows the variation of the relative intensities $\hat{\gamma}_i/\bar{\Gamma}_i$ with distance s along the trajectories in Figure 7. Here s is normalized on the nozzle radius R in order to provide the most revealing comparison with the single free jet. Equation (12) indicates that in the fully developed single jet, $\hat{\gamma}_c/\bar{\Gamma}_c = 0.24$, and the data in Figure 9 show that this value was approached only at values of s/R approaching 100. Thus the interacting jets were not fully developed in respect to $\hat{\gamma}_i/\bar{\Gamma}_i$ as they approached each other, and this fact alone would suggest a dependency of the results on the scale ratio $L/D \equiv L/2\,R$. However, it is also evident from Figure 9 that the jet interaction rapidly produces very high turbulence levels which should effectively overshadow any effects of upstream history. Downstream of the region of intensest interaction, the value of $\hat{\gamma}_i/\bar{\Gamma}_i$ falls with s and can be expected (see discussion in the following section) to asymptotically approach the value, around 0.24, to which the single jet tends at large s.

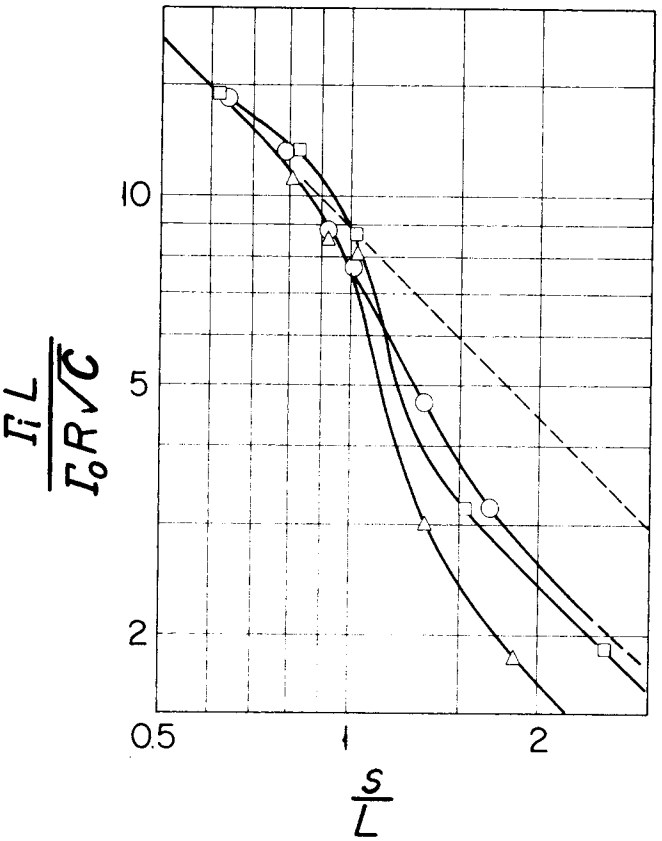

Fig. 8. Variation of mean concentration along the trajectory of the marked jet, one jet marked. The dashed line indicates the results for the single free jet, $\bar{\Gamma} \propto 1/s$. Half-angles of intersection, α: ○, 15 deg.; □, 30 deg.; and △, 45 deg.

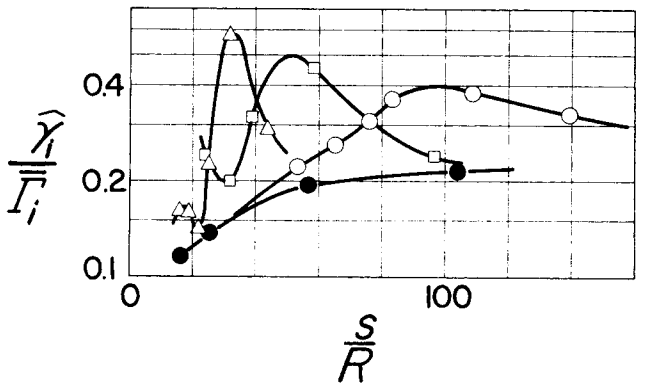

Fig. 9. Variation of the relative concentration fluctuation intensity along the jet trajectory, one jet marked. Half-angles of intersection, α: ○, 15 deg.; □, 30 deg.; and △, 45 deg. Single free jet: ●.

Far Downstream Behavior

Downstream of the interaction zone, after the two jets have merged, the resulting single jet is expected to exhibit a tendency towards an equilibrium structure in respect to turbulence and mean flow properties. The mean concentration on the x axis, $\bar{\Gamma}_c \equiv \Gamma(x, 0, 0)$, should thus, from what is generally known of jet behavior, tend towards a power-law decay with x

$$\bar{\Gamma}_c \propto (x - x_f)^{-n} \qquad (14)$$

where $(x, y, z) = (x_f, 0, 0)$ is the virtual origin of the jet in the final regime. The exponent n is 1 for round jets, as

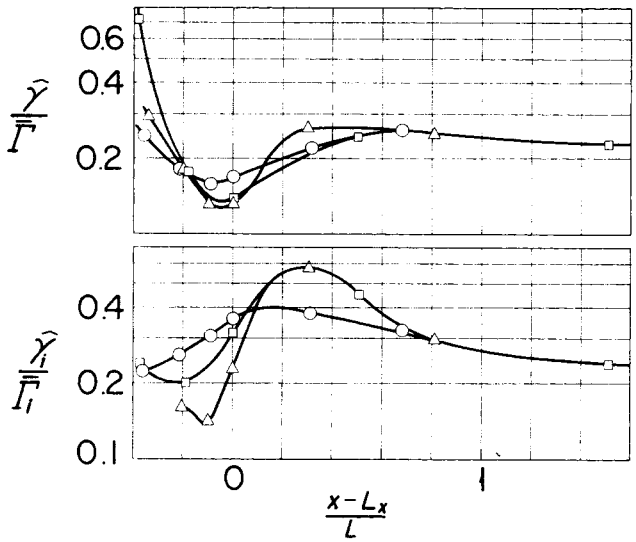

Fig. 10. Variation of relative concentration fluctuation intensity along the coordinate x axis (line of intersection of the planes of bilateral symmetry). Top *a*, both jets marked, and bottom *b*, one jet marked. Half-angles of intersection, α: ○, 15 deg.; □, 30 deg.; and △, 45 deg.

shown by Equation (10), and ½ for plane jets and 360 deg. fan jets (a 360 deg fan jet is generated by the present system in the case where the two source jets are directly opposed, $\alpha = 90$ deg.). The present investigation was, however, confined to the strong interaction zone, and the measurements would have to be extended much further downstream, roughly to $x = 10\,L$, in order to clearly define the tendency expressed by (14). The most that can be said is that Figure 8 shows a suggestion of settled behavior beyond $s/L = 1.5$, so the final regime is perhaps closely approached in this neighborhood.

It is further expected that the turbulence intensity should, in the final regime, tend towards the levels that are characteristic of well-developed free jets. This tendency, somewhat evident in Figure 9, is made very clear by Figure 10. Equation (12) indicates that on the center line of a fully developed round jet $\hat{\gamma}/\bar{\Gamma} = 0.24$, and the results of Becker et al. (1967*c*) give a similar value, 0.222. Velocity fluctuation intensities in plane jets are very similar to those in round jets, and we thus expect the same for $\hat{\gamma}/\bar{\Gamma}$. Furthermore, fan-shaped jets, which resemble plane jets in their behavior, should then also tend to have $\hat{\gamma}/\bar{\Gamma}$ around 0.22 to 0.24 on the center line far downstream. It therefore appears from Figure 10 that a more or less stable value of $\hat{\gamma}/\bar{\Gamma}$ is closely approached in the present system within the experimental range of x, and it is, as expected, about 0.22.

The direction of the approach of $\hat{\gamma}/\bar{\Gamma}$ towards equilibrium is interesting. In the ordinary single free jet, $\hat{\gamma}/\bar{\Gamma}$ grows with downstream distance, and this reflects the generation of turbulence kinetic energy in excess of the rate of dissipation until equilibrium is approached. In the present case there appears to be a superequilibrium level of turbulence energy remaining from the interaction zone, and this decays during the approach to equilibrium.

SUPERPOSITION PROPERTIES AND COMPLETENESS OF MIXING

The superposition property of the instantaneous marker concentration field is

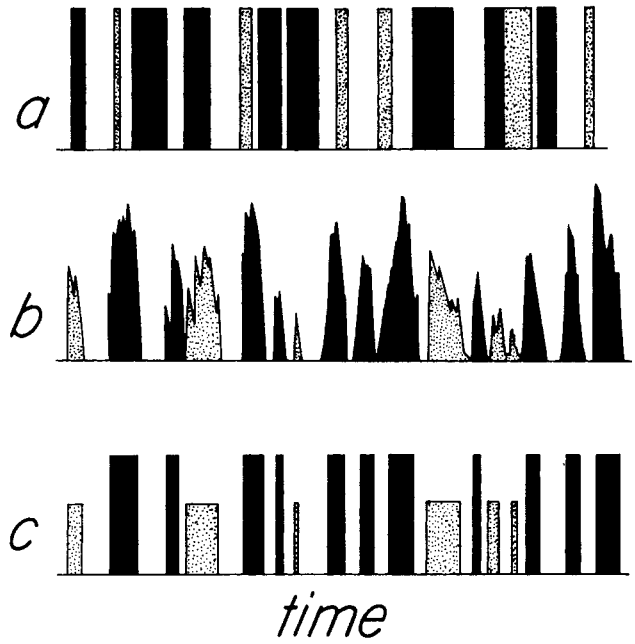

Fig. 11. Composition as a function of time, at two stages of mixing of three streams. Black, volume fraction of material from nozzle stream 1, and grey, volume fraction of material from nozzle stream 2. The remaining volume fraction consists of material entrained from the ambient fluid. Records: *a*, total segregation of all materials; *b*, total segregation of materials 1 and 2; and *c*, an approximation to *b*.

$$\Gamma = \Gamma_1 + \Gamma_2 \tag{15}$$

where Γ_1 is the field with one nozzle stream marked, Γ_2 is the field with the other nozzle stream marked, and Γ is the field when both are marked. It follows that

$$\bar{\Gamma} = \bar{\Gamma}_1 + \bar{\Gamma}_2 \tag{16}$$

$$\gamma = \gamma_1 + \gamma_2 \tag{17}$$

From (17)

$$\overline{\gamma^2} = \overline{\gamma_1^2} + 2\,\overline{\gamma_1\gamma_2} + \overline{\gamma_2^2} \tag{18}$$

and this shows that the mean-square values of the fluctuations are additive only if $\overline{\gamma_1\gamma_2}$ is zero. Attention is thus focused on the properties of the covariance function $\overline{\gamma_1\gamma_2}$ and the corresponding correlation function $R_{12} \equiv \overline{\gamma_1\gamma_2}/\hat{\gamma}_1\hat{\gamma}_2$. These functions have a key role in explaining the differences between the fields of $\overline{\gamma^2}$ and $\overline{\gamma_i^2}$, and it will be shown that they have fundamental significance in relation to the mixing process between the three streams entering the mixing field.

Theoretical Expectations

The mixing process between the three feed streams, the air from the two nozzles and the ambient air, is virtually isochoric (constant volume). Let G_1 denote the instantaneous volume fraction of air from nozzle 1 in the local mixture, G_2 the volume fraction of air from nozzle 2, and $G \equiv G_1 + G_2$ the volume fraction of air from both nozzles. The remainder, $G_3 \equiv 1 - G$, is the volume fraction of entrained ambient air. The corresponding fluctuating quantities are $g_1 = G_1 - \bar{G}_1$, $g_2 = G_2 - \bar{G}_2$, $g = G - \bar{G}$, and $g_3 = G_3 - \bar{G}_3$. We have

$$\left.\begin{aligned} G_1 + G_2 + G_3 &= 1 \\ \bar{G}_1 + \bar{G}_2 + \bar{G}_3 &= 1 \\ g_1 + g_2 + g_3 &= 0 \\ g &= -g_3 \end{aligned}\right\} \tag{19}$$

Suppose that material from the three feed streams is totally segregated at the considered point; in other words, mixing by molecular diffusion has been negligible. The record of G_1 and G_2 as a function of time then has the appearance shown in Figure 11*a*. Let subscript i denote any one of 1, 2, and 3. During a fraction of time equal to $\overline{G_i}$, $g_i = 1 - \overline{G_i}$, and during the remaining fraction $1 - \overline{G_i}$, $g_i = -\overline{G_i}$. Thus

$$\overline{g_i^2} = \overline{G_i}(1 - \overline{G_i})^2 + (1 - \overline{G_i})\overline{G_i}^2 = \overline{G_i}(1 - \overline{G_i}) \tag{20}$$

Consider, also, the covariance $\overline{g_i g_j}$ during a fraction of time equal to $\overline{G_i}$, $g_i = 1 - \overline{G_i}$ and $g_j = -\overline{G_j}$; during a fraction $\overline{G_j}$, $g_i = -\overline{G_i}$ and $g_j = 1 - \overline{G_j}$; and during a fraction $G_k = 1 - \overline{G_i} - \overline{G_j}$, $g_i = -\overline{G_i}$ and $g_j = -\overline{G_j}$. Thus

$$\overline{g_i g_j} = -\overline{G_i}\overline{G_j}(1 - G_i) - \overline{G_i}\overline{G_j}(1 - \overline{G_j}) + \overline{G_i}\overline{G_j}(1 - \overline{G_i} - \overline{G_j}) = -\overline{G_i}\overline{G_j} \tag{21}$$

The value of the correlation function

$$R_{ij}(g_i, g_j) \equiv \overline{g_i g_j}/\hat{g}_i\hat{g}_j \tag{22}$$

then follows from (20) and (21):

$$R_{ij} = -[\overline{G_i}\overline{G_j}/(1 - \overline{G_i})(1 - \overline{G_j})]^{1/2} \tag{23}$$

Equation (23) shows that, under the given conditions, R_{ij} is negative. When $\overline{G_i} << 1$ and $\overline{G_j} << 1$, $R_{ij} \simeq -\sqrt{(\overline{G_i}\overline{G_j})}$. When $\overline{G_k} << 1$, but $\overline{G_i}$ and $\overline{G_j}$ are both large, $1 - \overline{G_i} \simeq \overline{G_j}$ and $1 - \overline{G_j} \simeq \overline{G_i}$. Then $R_{ij} \simeq -1$.

Consider next the more interesting case, for the present problem, depicted in Figure 11*b*. This is the situation at the start of the interaction zone of the two-jet system where air from both nozzles has undergone micromixing with ambient air, but micromixing of the nozzle materials has barely begun. Figure 11*c* shows a crude model of the picture in Figure 11*b*, useful for a preliminary exploration. The signals G_1 and G_2 are represented as step functions with G_1 varying between zero and G_1' and G_2 between zero G_2'. Then, during a fraction of time equal to $\overline{G_i}/G_i'$, $g_i = G_i' - \overline{G_i}$, where $i = 1$ or 2, and during a fraction $1 - \overline{G_i}/G_i'$, $g_i = -\overline{G_i}$. We find that

$$\overline{g_i^2} = \overline{G_i}(G_i' - \overline{G_i}), \quad i = 1 \text{ or } 2 \tag{24}$$

$$\overline{g_1 g_2} = -\overline{G_1}\overline{G_2} \tag{25}$$

$$R_{12} = -[\overline{G_1}\overline{G_2}/(G_1' - \overline{G_1})(G_2' - \overline{G_2})]^{1/2} \tag{26}$$

Equations (24), (25), and (26) may be compared with (20), (21), and (23). The value of R_{12} is again seen to be negative. When $G_1' >> \overline{G_1}$ and $G_2' >> G_2$, $g_i^2 \simeq G_i G_i'$ and $R_{12} \simeq -\sqrt{(\overline{G_1}\overline{G_2}/G_1'G_2')}$. An interesting situation occurs when $1 - \overline{G_1}/G_1' - \overline{G_2}/G_2' << 1$, but neither of $\overline{G_1}/G_1'$ and $\overline{G_2}/G_2'$ is small compared to unity. This happens, crudely, in the middle of the start of the interaction zone, where each of the two merging jets is entraining fluid from the other, but very little ambient air. Then $1 - \overline{G_1}/G_1' \simeq \overline{G_2}/G_2'$ and $1 - \overline{G_2}/G_2' \simeq \overline{G_1}/G_1'$, and

$$\overline{g_i^2} \simeq \overline{G_i}\overline{G_j}, \quad i = 1 \text{ or } 2, \quad j = 1 \text{ or } 2, \quad i \neq j$$
$$\overline{g_1 g_2} = -\overline{G_1}\overline{G_2}$$
$$R_{12} \simeq -1$$

We can thus expect, in such a region, values of R_{12} approaching -1.

It may be noted that the model leading to (20), (21), and (23) involves the nozzle conditions ($G_1 = 1$ and $G_2 = 1$) and cannot be uncoupled from these. On the other hand, the second model, leading to (24), (25), and (26), is based entirely on local conditions and thus fits in with a generalized conception of the mixing field. This is another reason why the second model is more meaningful for the present problem.

We have just considered the situation at the start of the two-jet interaction zone. We will now examine the conditions to be expected far downstream of the interaction zone. There the material from the two nozzle streams will have become perfectly mixed, and the only process still occurring is the jet mixing of that mixture with fluid entrained from the surrounding field. Then, if $\dot{m}_1 \neq \dot{m}_2$, every where $G_1 \propto G_2$ and $g_1 \propto g_2$. It follows that $\overline{g_1 g_2} = \hat{g}_1\hat{g}_2$ and $R_{12} = 1$. When the nozzle streams are equal, $\dot{m}_1 = \dot{m}_2$, as in the present work, we also have $G_1 = G_2$ and $g_1 = g_2$.

It can thus be concluded that in the interaction zone of the present system, $-1 < R_{12} < 1$. At the start of the interaction zone, values of R_{12} approaching -1 may be observed. At the end of the interaction zone, R_{12} asymptotically approaches unity. It is clear that R_{12} can ultimately be regarded as a measure of the completeness of micromixing between material from the two nozzle streams; when $R_{12} = 1$, this mixing is complete.

The above argument has been given in terms of the gas mixing process, with volume fraction as the measure of composition. It has been demonstrated (Becker et al., 1969) that the smoke marker used in the present work provides a good representation of gas mixing fields, at least with respect to mean concentration and mean-square concentration fluctuations. If this is so, then $G_1 = \Gamma_1/\Gamma_o$ and $G_2 = \Gamma_2/\Gamma_o$. It follows that $\hat{g}_i/\overline{G_i} = \hat{\gamma}_i/\overline{\Gamma_i}$, and $R_{12} = \overline{\gamma_1\gamma_2}/\hat{\gamma}_1\hat{\gamma}_2$.

Observed Fields of R_{12}

The covariance $\overline{\gamma_1\gamma_2}$ must be evaluated from experimental values of $\overline{\gamma_1^2}$, $\overline{\gamma_2^2}$, and $\overline{\gamma^2}$ by means of Equation (18). The correlation function R_{12} is thus given by

$$R_{12} \equiv \frac{\overline{\gamma_1\gamma_2}}{\hat{\gamma}_1\hat{\gamma}_2} = \frac{1}{2}\,\frac{\overline{\gamma^2} - \overline{\gamma_1^2} - \overline{\gamma_2^2}}{\hat{\gamma}_1\hat{\gamma}_2} \tag{27}$$

In practice, the nozzle marker concentration Γ_o was generally not the same in different runs, and Equation (27) was therefore written in the working form

$$R_{12} = \frac{1}{2}\,\frac{\overline{\gamma^2}/\Gamma_o^2 - \overline{\gamma_1^2}/\Gamma_{1,o}^2 - \overline{\gamma_2^2}/\Gamma_{2,o}^2}{(\hat{\gamma}_1/\Gamma_{1,o})(\hat{\gamma}_2/\Gamma_{2,o})} \tag{28}$$

where $\Gamma_{1,o}$ is the smoke concentration in the nozzle stream 1 when only that stream is marked, $\Gamma_{2,o}$ is the concentration in stream 2 when only it is marked, and Γ_o is the concentration in both streams when both are marked.

The calculated profiles of R_{12} for $\alpha = 30$ deg. are shown in Appendix A.* The values of R_{12} range from close to -1 at the beginning of the interaction zone to 1 at the end, as expected. The results, as in the case of $\overline{\Gamma_i}$, $\hat{\gamma}_i$, $\overline{\Gamma}$, and $\hat{\gamma}$, are too sparse to allow the construction of contour maps. The results for $\alpha = 15$ and 45 deg. are, however, sufficiently dense. The contour map for $\alpha = 45$ deg. is shown in Figure 12, and that for $\alpha = 15$ deg. is in Appendix A.*

Since R_{12} is a measure of the completeness of micromixing between material from the two nozzle streams, a most

* See footnote on p. 953.

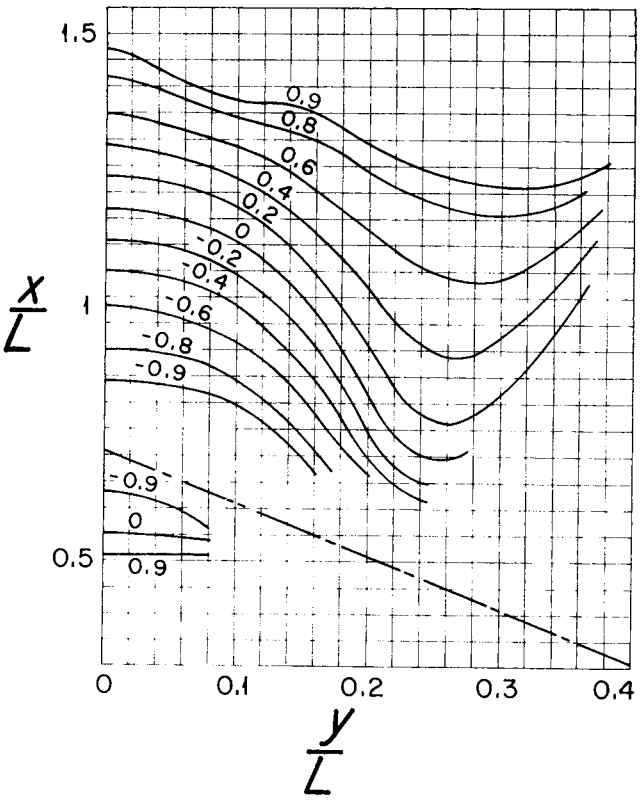

Fig. 12. Field of the correlation function $R_{12} \equiv \overline{\gamma_1\gamma_2}/\hat{\gamma}_1\hat{\gamma}_2$ for $\alpha =$ 45 deg. The dash-dotted line indicates the nozzle axes.

revealing picture of the mixing process emerges from these diagrams. At $\alpha = 45$ deg., a well-mixed recirculation zone is evident in the pinch between the jets at the start of the interaction zone. Completion of mixing is apparently approached last along the x axis, and Figure 13 shows, for all values of α, the interesting relation there between R_{12} and $(x - L_x)/L$. The interactive mixing process is evidently completed over a distance only a little greater than L, roughly in the region $L_x < x < L_x + L$.

CONCLUSION

It is evident that the covariance between concentration fluctuations in the material from two feed streams written $\overline{\gamma_1\gamma_2}$ and $\overline{g_1g_2}$ at various stages in the preceding discussion, together with the associated correlation function R_{12}, is generally significant for mixing fields entered by three or more feed streams. This covariance necessarily enters into the mathematical formulation of such problems, and a transport equation for it is an element of the basic set of governing equations. A derivation of this transport equation is given in Appendix A.* Some general aspects of mathematical simulation and prediction procedures are also discussed there, and the role of $\overline{g_1g_2}$ and R_{12} in chemical reactions is examined.

The quantity $\overline{g_1g_2}/\overline{G}_1\overline{G}_2$ is a form of the intensity of segregation defined by Danckwerts (1953). We have shown that, in the context of the present problem, it is -1 in total segregation and becomes positive as the mixing process between the two finite feed streams is completed. The same quantity has a somewhat different behavior when applied to mixing fields entered by only two streams. We have then, in constant-volume mixing, $g_2 = -g_1$ and $\overline{G}_2 = 1 - \overline{G}_1$. Here $\overline{g_1g_2}/\overline{G}_1\overline{G}_2$ is always

* See footnote on p. 953.

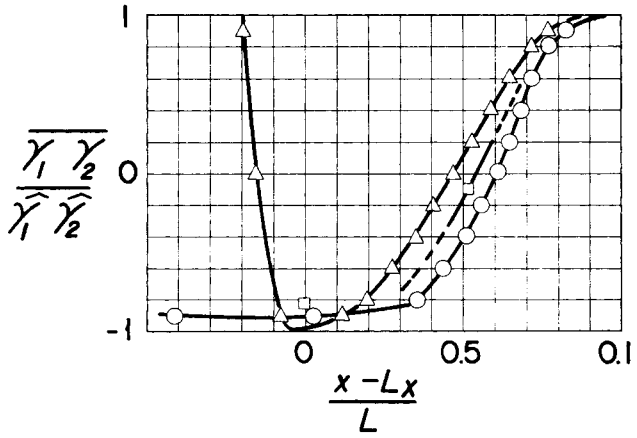

Fig. 13. Variation of the correlation function R_{12} along the coordinate x axis (line of intersection of the planes of bilateral symmetry). Half-angles of intersection, α: ○, 15 deg.; □, 30 deg.; and △, 45 deg.

negative, has the value -1 in total segregation, and if both feed streams are finite, goes to zero as mixing is completed. The behavior of $\overline{g_1g_2}/\overline{G}_1\overline{G}_2$ in the present context is considerably less interesting that of $R_{12} = \overline{g_1g_2}/\hat{g}_1\hat{g}_2$, and so we have not pursued it.

The characteristic length scale L used in the present work is convenient and significant for the range of the angle α that was covered, and generally for $\alpha > 0$ and not small. When α is near zero or negative, however, L is inappropriate or undefined, and the scale L_y (one-half the distance between the virtual jet origins) should be adopted. In the general two-jet problem, the most generally serviceable scale (always appropriate) is the distance between the nozzle centers.

ACKNOWLEDGMENT

The work was supported by grants from the National Research Council of Canada. The results were first reported in an M.Sc. thesis (Booth, 1971). One author (HAB) is grateful to Professor J. M. Beér and his university for facilities enjoyed during a sabbatical leave in the Department of Chemical Engineering at the University of Sheffield.

NOTATION

b = characteristic radius of the single round free jet with respect to the mean concentration field; $r = b$ at $\overline{\Gamma}(x, r) = (\frac{1}{2})\,\overline{\Gamma}(x, 0)$
C = constant, $C \equiv 0.853$ K
D = nozzle diameter
$\mathcal{D}$ = material diffusivity, gas in gas
G_1, G_2 = volume fractions of air from nozzle streams 1 and 2
G = $\equiv G_1 + G_2$
G_3 = volume fraction entrained ambient air
g_1, g_2, g_3, g = turbulent fluctuations in G_1, G_2, G_3, G
I_o = momentum flux from either nozzle
J_o = smoke flux from either nozzle
K = momentum shape factor, nozzle velocity profile
L = characteristic length scale of interacting jet system, distance from virtual origin of either jet to the point of intersection of the nozzle axes
L_x, L_y = auxiliary length scales, the x and y components of L
L_{12} = center-to-center distance between nozzle mouths
$\dot{m}_o$ = mass flux from either nozzle, when these are equal
$\dot{m}_1$, $\dot{m}_2$ = mass fluxes from nozzles 1 and 2, general case ($\dot{m}_o$ is used when $\dot{m}_1 = \dot{m}_2$)

r = radial position, cylindrical coordinates, in single free jet
$\mathbf{r}$ = position vector
R = $\equiv D/2$, nozzle radius
R_{ij} = correlation function for fluctuations in the concentrations of components i and j
R_{12} = correlation function for fluctuations in the concentration of material from nozzle streams 1 and 2
s = distance along the jet trajectory, from the virtual origin
U_o = mean discharge velocity at nozzle
U^* = characteristic velocity scale of the interacting jets system, Equation (3)
x, y, z = Cartesian coordinates of the interacting jet system, Figure 1*b*
x_f = virtual origin of the combined jet downstream of the interaction zone

Greek Letters

α = one-half the angle between the jet nozzle axes
Γ = total smoke concentration; $\Gamma \equiv \Gamma_1 + \Gamma_2$
Γ_1, Γ_2 = concentration of smoke from nozzle streams 1 and 2
Γ_i = concentration of smoke from either nozzle stream
$\gamma, \gamma_1, \gamma_2, \gamma_i$ = turbulent fluctuations in $\Gamma, \Gamma_1, \Gamma_2, \Gamma_i$
ϵ = rate of viscous dissipation of turbulent kinetic energy, per unit mass of fluid
κ = $\equiv 2\pi f/\overline{U}_x$, wave number
ν = kinematic viscosity
ρ = density

Subscripts

c = value on the x axis ($y = 0$ and $z = 0$)
i = value when one of the jet nozzle streams is marked with smoke
i, j, k = material of feed streams i, j, and k
0 = value in nozzle stream
1, 2 = smoke from nozzle streams 1 and 2
1, 2, 3 = material of feedstreams 1, 2, and 3

Superscripts

$(\overline{})$ = time-mean value
$(\wedge)$ = root-mean-square value; $\hat{\gamma} \equiv \sqrt{\overline{(\gamma^2)}}$

Dimensionless Parameters

Ma = $\equiv U_o/c$, Mach number
Re = $\equiv U_oD/\nu$, Reynolds number
Sc = $\nu/\mathcal{D}$, Schmidt number for gas in gas

LITERATURE CITED

Baron, T., and E. H. Bollinger, "Mixing of High Velocity Air Jets," Tech. Rept. No. CML-3, Engineering Experimental Station, University of Illinois (1952).

Becker, H. A., H. C. Hottel, and G. C. Williams, Mixing and Flow in Ducted Turbulent Jets," *Ninth Symposium (International) on Combustion,* pp. 7-20, Academic Press New York (1963*a*).

————, "Concentration Intermittency in Jets," *Tenth Symposium (International) on Combustion,* pp. 1253-1263, Academic Press, New York (1965).

————, "Concentration Fluctuations in Ducted Turbulent Jets, *Eleventh Symposium (International) on Combustion,* pp. 791-798, Academic Press, New York (1967*a*).

————, "On the Light Scatter Technique for the Study of Turbulence and Mixing," *J. Fluid Mech.,* **30,** 259-284 (1967*b*).

————, "The Nozzle-Fluid Concentration Field of the Round, Turbulent, Free Jet," *ibid.,* 285-303 (1967*c*).

Becker, H. A., R. E. Rosensweig, and J. R. Gwozdz, "Turbulent Dispersion in a Pipe Flow," *AIChE J.,* **12,** 964-971 (1966).

Booth, B. D., *"Mixing in Intersecting Turbulent Jets,"* M.Sc. thesis, Queen's University, Kingston, Ontario, Canada (1971).

Danckwerts, P. V., "The Definition and Measurement of Some Characteristics of Mixtures, *Appl. Sci. Res.,* A3, 279-296 (1953).

Kirillov, V. A., and B. G. Khudenko, "Calculation of the Direction of the Axis of a Stream Resulting from the Mixing of Turbulent Jets," *J. Eng. Phys.,* **9,** 414-415 (1965).

Makarov, I. S., and B. G. Khudenko, "Mixing of Intersecting Turbulent Jets," *ibid.,* **8,** 304-306 (1965).

Rosensweig, R. E., H. C. Hottel, and G. C. Williams, "Smoke-Scattered Light Measurements of Turbulent Concentration Fluctuations," *Chem. Eng. Sci.,* **15,** 111-129 (1961).

Rummel, K., *Der einfluss des Mischvorganges auf die Verbrennung von Gas and Luft in Feuerungen,* Verlag Stahleisen, Dusseldorf (1937).

Supplementary material has been deposited as Document No. 02679 with the National Auxiliary Publications Service (NAPS), c/o Microfiche Publications, 440 Park Ave. South, New York, N. Y. 10016 and may be obtained for $1.50 for microfiche or $5.00 for photocopies.

Manuscript received February 27, 1975; revision received May 27, and accepted May 28, 1975.

Nonlinear Theory of Free Coating onto a Vertical Surface

The work of Landau and Levich (1942) initiated detailed theoretical and experimental study of the flow of the thin liquid film entrained by a steady withdrawal of a sheet from a bath of liquid. The existing theories, which differ considerably, are all based on linearization of the problem and give single relationships between film thickness T and a capillary number Ca. The present paper demonstrates theoretically that differing physical properties for each liquid result not in a single curve but in a family of curves for T vs. Ca and that the complete set of previous experimental work required and fitted the family of curves. Previous theories could fit only a portion of this experimental data.

The solution requires a nonlinear theory to include inertial terms and two-dimensional flow and thus treat the parameter of liquid physical properties. This is obtained by applying a nonlinear approach based on the direct method of Galerkin. Owing to the nonlinear character of the solution, the new theory has the advantage of accurately determining the shape and size of the upper meniscus profile. Excellent agreement with the complete set of available experimental data is obtained.

M. NABIL ESMAIL

and

RICHARD L. HUMMEL

Department of Chemical Engineering and Applied Chemistry
University of Toronto
Toronto, Ontario